Chinese Chemical Letters 32 (2021) 493–496

Contents lists available at ScienceDirect

Chinese Chemical Letters

journal homepage: www.elsevier.com/locate/cclet

Communication

Stimuli-responsive cyclometalated platinum complex bearing bent molecular geometry for highly efficient solution-processable OLEDs

Zhenhua Wei[a,d,1], Kai Zhang[a,1], Chan Kyung Kim[c,1], Shuai Tan[a,d], Shaojie Wang[b,f], Lin Wang[b,f,*], Jun Li[e], Yafei Wang[a,**]

[a] National Experimental Demonstration Center for Materials Science and Engineering (Changzhou University), Jiangsu Collaborative Innovation Center of Photovoltaic Science and Engineering, Jiangsu Engineering Laboratory of Light-Electricity-Heat Energy-Converting Materials and Applications, School of Materials Science & Engineering, Changzhou University, Changzhou 213164, China
[b] Center for High Pressure Science (CHiPS), State Key Laboratory of Metastable Materials Science and Technology, Yanshan University, Qinhuangdao 066004, China
[c] Department of Chemistry and Chemical Engineering, Inha University, Incheon 22212, South Korea
[d] College of Chemistry, Xiangtan University, Xiangtan 411105, China
[e] School of Chemical Engineering and Technology, North University of China, Taiyuan 030051, China
[f] Center for High Pressure Science and Technology Advanced Research, Shanghai 201203, China

HPSTAR 1140-2021

ARTICLE INFO

Article history:
Received 16 March 2020
Received in revised form 24 April 2020
Accepted 6 May 2020
Available online 12 May 2020

Keywords:
Stimuli responsive emission
Platinum complex
Solution-processable OLEDs
Synthesis and property

ABSTRACT

Smart materials, such as stimuli-responsive luminescence, have attracted much attentions due to their potential application in semiconductor filed. In this context, platinum complexes of (dfppy-DC)Pt(acac) and (dfppy-*O*-DC)Pt(acac) were prepared and characterized, in which (2-(4',6'-difluorophenyl)pyridinato-*N*,C2')(2,4-pentanedionato-*O*,*O*)Pt(II) was used as the planar emission core and 9-(4-(phenylsulfonyl) phenyl)-9*H*-carbazole (DC) was regard as the bent pendent. Both platinum complexes showed bright emission in solution and solid state, concomitant with charming external-stimuli-responsive emission under mechanical grinding, organic solvent vapors and pressure. The change emission color spanned from yellow to near-infrared region. Using the platinum complexes as the dopant, solution processable organic light-emitting diodes (OLEDs) were fabricated and a maximum external quantum efficiency of ~18% was achieved, which is the highest value among the reported solution-processable OLEDs based on external-stimuli-responsive luminescence. This research demonstrated that platinum complex can show promising stimuli responsive emission *via* ingenious molecular design, indicating a novel way for developing the smart materials in semiconductor filed.

Since the pioneer work of Forrest *et al.* in 1998 [1], cyclometalated platinum complex has become a research hotspot in organic light-emitting diodes (OLEDs) due to its intrinsic planar structure, theoretical 100% internal quantum efficiency and rich emissive characteristic (metal-to-ligand charge transfer, ligand-to-ligand charge transfer, metal-metal-to-ligand charge transfer, *etc.*) [2]. Over the past several decades, considerable cyclometalated-platinum complexes spanning from blue emission to near-infrared emission have been developed with very high external quantum efficiency of >20% in OLEDs [3].

As we know, the unique square-planar structure and strong intermolecular Pt-Pt interaction play a crucial role in the luminescent property of platinum complex [4]. This feature of platinum complex was also extensively employed as stimuli-responsive materials showing the varied emission color dependent on the π-π/or Pt-Pt distance [5], which has attracted much attention by researchers recently because of their promising applications in organic semiconductor [6]. Generally, the strategy for the stimuli-responsive platinum complex adopted planar *N*-containing heterocyclic ligand, such as azole, bipyridine, and pincer ligand (Fig. 1) [6,7]. Few platinum complexes bearing acetylacetone ligand exhibited emission color changed with external-stimuli conditions. In addition, due to the emission quenching by the rigid and planar structural, little stimuli-responsive platinum complexes were employed as an emitter in

* Corresponding author at: Center for High Pressure Science (CHiPS), State Key Laboratory of Metastable Materials Science and Technology, Yanshan University, Qinhuangdao 066004, China.
** Corresponding author.
E-mail addresses: wanglin@hpstar.ac.cn (L. Wang), qiji830404@hotmail.com (Y. Wang).
[1] These authors are contributed equally to this work.

https://doi.org/10.1016/j.cclet.2020.05.005

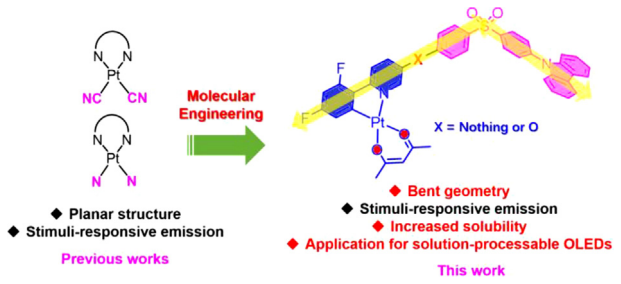

Fig. 1. Molecular strategy for the platinum complex.

OLEDs, let alone solution-processable OLEDs. Chi *et al.* reported a platinum complex based on pyrazole chelate which showed mechanoluminescence and concentration dependent photoluminescence. Using this platinum complexes as the emitter, the OLEDs fabricated *via* vacuum deposition showed a blue emission with the maximum external quantum efficiency (*EQE*) of 9.1% [8]. Therefore, there is an urgent need to explore novel platinum complexes which can show external stimuli luminescence response and definitely have a promising application in solution-processable OLEDs.

To solve this issue, herein, we proposed that the molecule should not only possess planar structure but also have appropriate steric hindrance, in which the planar moiety can possess good intermolecular π-π interaction and the steric hindrance affects the molecular packing, probably in favor of the external stimuli, such as pressure and grinding (Fig. 1). On the other hand, the steric structure has a positive effect on suppressing the emission quenching in solid state and increasing the solubility, implying a promising application in solution processable OLEDs. With these in mind, we employed the typical platinum complex of (dfppy)Pt(acac)[(2-(4',6'-difluorophenyl)pyridinato-N,C2′2′)(2,4-pentanedionato-*O,O*)Pt(II)] as the emission core, which has a square-planar structure. Then a second emissive fragment of 9-(4-(phenylsulfonyl)phenyl)-9*H*-carbazole (DC) bearing bent shape was introduced into the cyclometalating ligand (Fig. 2). In order to further explore the molecular structure-property relationship, an oxygen atom was integrated between the platinum complex-based emission core and the DC moiety, probably playing a crucial role on the molecular packing. To prove our hypothesis, two platinum complexes of (dfppy-DC)Pt(acac) and (dfppy-*O*-DC)Pt(acac)bearing bent shape were prepared and characterized, and their structure-property relationship was explored systematically.

As shown in Scheme S1 (Supporting information), both platinum complexes were synthesized and confirmed by ^{1}H NMR, TOF-MS and X-ray crystal diffraction. Single crystals of the platinum complexes were obtained from chloroform/methanol solution and confirmed by X-ray crystallography. As expected, both platinum complex moieties are square planar geometry (Fig. 2), while the DC fragment showed a twist configuration with the dihedral angels (between carbazole and diphenyl sulfone) of 59.97° and 57.12° in (dfppy-DC)Pt(acac) and (dfppy-*O*-DC)Pt(acac), respectively (Tables S1 and S2 in Supporting information). The platinum complexes also form a charming crystal stacking and relatively large distance of Pt···Pt (Figs. S1 and S2 in Supporting information).

The platinum complexes show two main absorption bands between 300 and 550 nm (Figs. S3 and S4 in Supporting information). The absorption band at about 337 ± 1 nm is assigned to the π-π^* transition of the aromatic ring, while the absorption bands in the range of 350–450 nm are attributed to the mixture of metal-to-ligand charge transfer (MLCT) and intraligand charge transfer (ILCT) transitions. Compared to (dfppy-*O*-DC)Pt(acac), (dfppy-DC)Pt(acac) exhibits a clearly red-shifted absorption spectrum owing to its extended conjugation. The DFT results reveal that the 9-phenylcarbazole moiety makes the major contribution to the highest occupied molecular orbitals (HOMO) for both platinum complexes. The lowest unoccupied molecular orbitals (LUMO) mainly localizes at 2,4-difluorophenylpyridine, diphenyl sulfone and platinum atom (Fig. S5 in Supporting information). Obviously, the integrated oxygen atom shows a negligible effect on HOMO and LUMO patterns.

With the excitation wavelength of 360 nm, the photoluminescence (PL) of both platinum complexes present clearly dual emissions in degassed toluene solution at room temperature (Fig. 3). The weak emission bands at short-wavelength (*ca.* 412 nm and 437 nm) can be contributed to the phenylpyridine-diphenyl sulfone-carbazole fragment, whereas the intense and broad structured emission bands in the long wavelength (480–600 nm, Table S3 in Supporting information) are contributed to a mixture of MLCT and ligand center transitions of the platinum complexes [9]. Compared to (dfppyPt-DC)Pt(acac), complex (dfppyPt-*O*-DC)Pt(acac) exhibits a distinct blue-shifted emission spectrum in long-wavelength due to the destroyed π conjugation. It is noted that a short luminescence decay profiles of nanosecond was found for the emission bands between 410 nm and 440 nm and a long lifetime of microsecond was detected for the emission bands at long-wavelength (Table S3), implying fluorescence and phosphorescence, respectively. In degassed toluene solution, satisfied photoluminescent quantum yields (*PLQY*) of 58% and 18% were achieved for complexes (dfppyPt-DC)Pt(acac) and (dfppyPt-*O*-DC)Pt(acac), respectively. Based on the lifetime and *PLQY*, the radiative rate constant (k_r) were calculated to be $5.40 \times 10^5\ s^{-1}$ and $3.62 \times 10^5\ s^{-1}$ and the nonradiative rate constant (k_{nr}) were evaluated to be $4.07 \times 10^5\ s^{-1}$ and

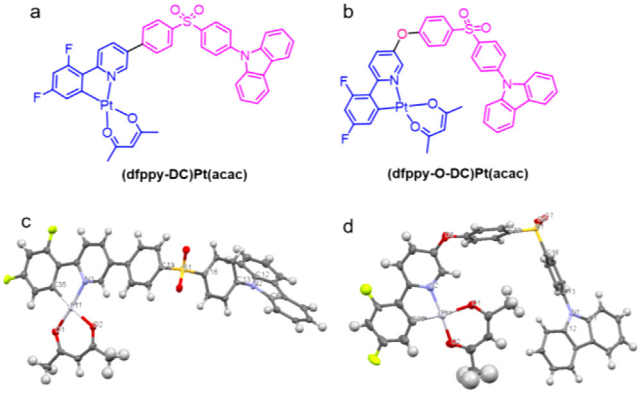

Fig. 2. The molecular structures (a and b) and crystal structures (c and d, hydrogen atoms are omitted).

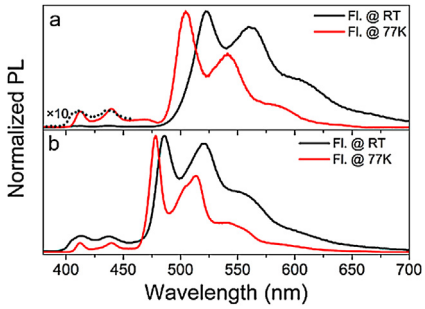

Fig. 3. Fluorescent and phosphorescent emission spectra of platinum complexes in toluene solution (10^{-5} mol/L) with the excitation wavelength of 360 nm: (a) (dfppy-DC)Pt(acac), the dot line is 10 times of fluorescence at room temperature between 380 nm and 460 nm; (b) (dfppy-*O*-DC)Pt(acac).

$1.65 \times 10^6\ s^{-1}$ for complexes (dfppyPt-DC)Pt(acac) and (dfppyPt-*O*-DC)Pt(acac), respectively (Table S3). Definitely, complex (dfppyPt-*O*-DC)Pt(acac) presents a sky-blue emission with relatively low *PLQY* due to the very large k_{nr}. At 77 K, both platinum complexes in degassed toluene solution show analogous emission spectra with those of at room temperature (Fig. 3). However, the characteristic hypsochromic shift of the low-temperature PL spectra in freeze is observed for both platinum complexes at long-wavelength, probably due to the motional relaxation of the excited-state geometry which is prone to be affected by the rigidity of the matrix [10]. On the other hand, negligible change for the emission bands at short-wavelength suggests it could be attributed to the ligand center transitions.

Due to the interesting molecular packing in crystal, we put insight into the emission property under applying external conditions, such as grinding and fuming. As expected, (dfppy-DC)Pt(acac) showed charming mechanochromic luminescence-properties. The PL spectra of the solid samples under different stimuli and the photographs under UV light are shown in Fig. 4. Compared to the PL profile in solution, (dfppy-DC)Pt(acac) presents a red-shifted emission spectrum with a maximum emission peak centered at 573 nm and a shoulder of 538 nm in pristine sample, which can be explained by the strong molecular aggregation in solid state. At the same time, the powder XRD (PXRD) pattern displays a lot of intense and sharp diffraction peaks in the range of 5°–60° (Fig. 4b), implying micro-crystalline structure in pristine state. Grinding the sample with pestle in a mortar, distinct red shift with a maximum emission peak at 637 nm is observed (Fig. 4a). It can be attributed to the decreased Pt-Pt distance, and leading to metal-metal-to-ligand charge transfer (MMLCT) transitions [11]. Therefore, the molecular stacking in ground state should be closer than that of pristine state (Fig. S6 in Supporting information). As for the PXRD patterns in ground state, all the intense and sharp diffraction peaks in pristine state are disappeared, while some weak and broad diffraction peaks turn out. This change in the PXRD pattern demonstrates that (dfppy-DC)Pt(acac) is transformed to partially amorphous aggregates after grinding [11], which is also responsible for the emission color change. After fuming in dichloromethane vapor for 15 min, the emission profile almost recovers to that of pristine state. However, the emission band at about 620 nm still exists after fuming, probably due to the molecular state assessed as neither too tight nor too loose (Fig. S6). Similarly, the PXRD pattern of fuming with intense and sharp diffraction peaks is well match with that of pristine, implying that a micro-crystalline structure is obtained after fuming. Obviously, the mechanochromism luminescence behavior of this platinum complex is ascribed to the Pt-Pt distance and intermolecular interaction. Unfortunately, we did not find the mechanochromic luminescence for (dfppy-*O*-DC)Pt(acac) after grinding, probably due to the different molecular aggregation in crystal which is insensitive to the mechanical grinding.

To further investigate the effect of molecular packing in the crystal on the luminescence, hydrostatic pressure-dependent luminescence of both platinum complexes was carried out at room temperature *via* diamond anvil cell (DAC) equipment (Fig. 5 and Fig. S7 in Supporting information). The crystal (recrystallization from $CH_3OH/CHCl_3$, the same below) of (dfppy-DC)Pt(acac) shows structured emission with a maximum emissive peak at 578 nm with the shoulders at about 532, 619 and 681 nm under ambient condition. When the pressure was gradually increased from 1 atm to 20 GPa, the emissive intensity gradually decreases, probably due to the stronger intermolecular interaction leading to increased non-radiative transition. Simultaneously, the emissive spectra present obviously red shift with the increase of pressure. The maximum emissive peak is from 578 nm at 1 atm to 690 nm at 19.91 GPa, implying the colors of the crystal underwent a remarkable change from green to near-infrared with the increase of pressure. As shown in Fig. 5, the visualized colors of the samples at different pressures can also illustrate the changed emission profiles. This red-shifted emission can be explained by the shorter distance of the adjacent platinum centers. According to the previous reports [10,12], the distance between Pt-Pt decreases with increasing pressure generating to an destabilized valence band due to the overlap of the d_z^2 HOMO orbitals from all platinum centers, whereas the vacant p_z orbital of adjacent platinum centers start to overlap and form a stable conduction band, leading to the drastic decrease in the luminescence energy. Compared to (dfppy-DC)Pt(acac), complex (dfppy-*O*-DC)Pt(acac) exhibits an analogous piezochromism luminescence behavior. The variation tendency of (dfppy-*O*-DC)Pt(acac) in emissive peak and intensity under the pressure change is the same with that of (dfppy-DC)Pt(acac). At ambient pressure, (dfppy-*O*-DC)Pt(acac) shows a structureless emissive band centered at 608 nm. When the pressure is 5.4 GPa, the spectrum shows a clearly additional emissive band at about 857 nm. In addition, the emissive intensity at ~850 nm gradually increases with the increasing pressure, probably due to the increased MMLCT effect with the decreased Pt-Pt distance.

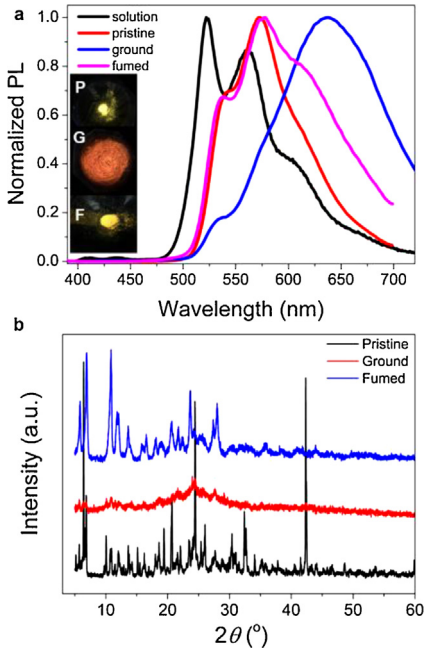

Fig. 4. PL spectra (a) and powder XRD patterns (b) of (dfppy-DC)Pt(acac) in different state at room temperature. Insert: Images of (dfppy-DC)Pt(acac) under UV light with 365 nm (P: pristine; G: ground; F: fumed).

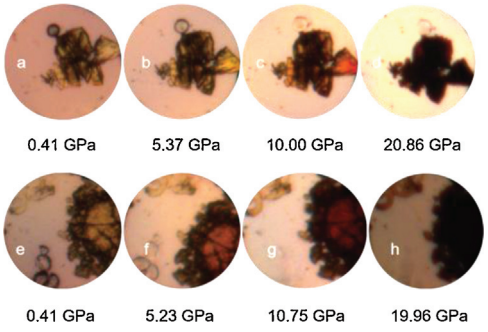

Fig. 5. Pictures of platinum complexes during the pressurizing process at room temperature, (a–d) (dfppy-DC)Pt(acac), (e–h) (dfppy-*O*-DC)Pt(acac).

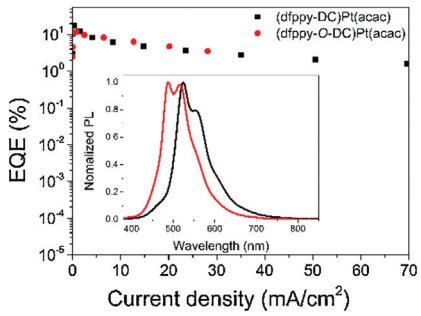

Fig. 6. The current density-*EQE* curves of the devices with 5 wt% dopant concentration. Insert: the EL spectra of the devices.

Obviously, introduction of oxygen atom apparently plays a key role in the external-stimuli-responsive emission.

To evaluate the electroluminescent property, solution-processable OLEDs were fabricated (Fig. S8 in Supporting information). The electroluminescent (EL) spectra and external quantum efficiency (*EQE*)-current density curves of the devices are shown in Fig. 6. The EL spectra, similar with the PL profiles, exhibit the maximum emission peaks at 488 nm and 524 nm for (dfppy-DC)Pt(acac) and (dfppy-*O*-DC)Pt(acac), respectively, implyingthat the emissions are dominated from the platinum complexes. In addition, the disappeared emission from CzAcSF means that there is a complete energy transfer from the host to the dopant. The Commission Internationale de L'Eclairage (CIE) are (0.33, 0.56) and (0.22, 0.45) for (dfppy-DC)Pt(acac) and (dfppy-*O*-DC)Pt(acac)-based devices, respectively. As shown in Fig. S9 (Supporting information), the (dfppy-DC)Pt(acac) based device shows a turn-on voltage ($V_{turn\text{-}on}$, at 1.0 cd/m^2) of 4.0 V, while the device based on complex (dfppy-*O*-DC)Pt(acac) has a lower $V_{turn\text{-}on}$ of 2.8 V. Due to the smaller k_{nr} and higher PLQY, (dfppy-DC)Pt(acac)-based device possesses better performances with a highest *EQE* of 17.79%, current efficiency (*CE*) of 58.31 cd/A and luminance of 5463 cd/cm^2. The (dfppy-*O*-DC)Pt(acac)-based device show a maximum *EQE* of 13.47%, current efficiency (*CE*) of 38.45 cd/A and luminance of 2861 cd/cm^2. Increased with the dopant concentration, the devices present inferior performances with decreased *EQE* due to the concentration quenching.

In summary, two novel cyclometalated platinum complexes with bent geometry were synthesized and characterized. The intermolecular interaction was varied and dependent on the external stimulus which results in the changed emission color from green to near-infrared region for the platinum complexes. Compared to the previous reports, this bent geometry based cyclometalated platinum complexes showed universal external-stimuli-responsive emission. The mechanism of external-stimuli-responsive emission implied that the distances of the π-π planar and platinum center are the responsible for the change in the emission profiles. Employing both platinum complexes as the dopant in solution-processable OLEDs, a maximum external quantum efficiency of ~18% was achieved which is among the highest efficiency for the devices based on external-stimuli-responsive materials. This research demonstrated that an elaborate regulation on molecular geometry would be an effective method for designing smart materials.

Declaration of competing interest

The authors declare that they have no known competing financial interests or personal relationships that could have appeared to influence the work reported in this paper.

Acknowledgments

Financial support was from the National Natural Science Foundation of China (Nos. 51773021, 51911530197, U1663229), Six Talent Peaks Project in Jiangsu Province (No. XCL-102), the Talent Project of Jiangsu Specially-Appointed Professor, Natural Science Fund for Colleges and Universities in Jiangsu Province (No. 19KJA430002).

Appendix A. Supplementary data

Supplementary material related to this article can be found, in the online version, at doi:https://doi.org/10.1016/j.cclet.2020.05.005.

References

[1] M.A. Baldo, D.F. O'Brien, Y. You, et al., Nature 395 (1998) 151–154.
[2] (a) M. Chaaban, C. Zhou, H. Lin, B. Chyi, B. Ma, J. Mater, Chem. C 7 (2019) 5910–5924;
(b) C. Fan, C. Yang, Chem. Soc. Rev. 43 (2014) 6439–6469;
(c) X. Yang, G. Zhou, W.Y. Wong, Chem. Soc. Rev. 44 (2015) 8484–8575.
[3] (a) J. Zhao, Z. Feng, D. Zhong, et al., Chem. Mater. 30 (2018) 929–946;
(b) Z. Zhu, C. Park, K. Klimes, J. Li, Adv. Opt. Mater. 7 (2019) 1801518;
(c) K. Kim, J. Liao, S.W. Lee, et al., Adv. Mater. 28 (2016) 2526–2532.
[4] (a) S. Yang, F. Meng, X. Wu, et al., J. Mater. Chem. C 6 (2018) 5769–5777;
(b) S. Tan, X. Wu, Y. Zheng, Y. Wang, Chin. Chem. Lett. 30 (2019) 1951–1954.
[5] (a) K. Li, Y. Chen, W. Lu, N. Zhu, C.M. Che, Chem. Eur. J. 47 (2011) 4109–4112;
(b) J. Ni, X. Zhang, Y.H. Wu, L.Y. Zhang, Z.N. Chen, Chem. Eur. J. 47 (2011) 1171–1183.
[6] (a) Y. Shigeta, A. Kobayashi, M. Yoshida, M. Kato, Inorg. Chem. 58 (2019) 7385–7392;
(b) A. Kobayashi, H. Hara, T. Yonemura, H.C. Chang, M. Kato, Dalton Trans. 41 (2012) 1878–1888;
(c) O.S. Wenger, Chem. Rev. 113 (2013) 3686–3733;
(d) Q. Zhao, F. Li, C. Huang, Chem. Soc. Rev. 39 (2010) 3007–3030.
[7] (a) C. Cuerva, J.A. Campo, M. Cano, C. Lodeiro, Chem. Eur. J. 22 (2016) 10168–10178;
(b) K. Ohno, Y. Kusano, S. Kaizaki, A. Nagasawa, T. Fujihara, Inorg. Chem. 57 (2018) 14159–14169;
(c) X. Zhang, J.Y. Wang, J. Ni, L.Y. Zhang, Z.N. Chen, Inorg. Chem. 51 (2012) 5569;
(d) S. Carrara, A. Aliprandi, C.F. Hogan, L. De Cola, J. Am. Chem. Soc. 139 (2017) 14605–14610.
[8] L. Huang, G. Tu, Y. Chi, et al., J. Mater. Chem. C 1 (2013) 7582–7592.
[9] M. Han, Y. Tian, Z. Yuan, L. Zhu, B. Ma, Angew. Chem. Inter. Ed. 53 (2014) 10908–10912.
[10] Y. You, K.S. Kim, T.K. Ahn, D. Kim, S.Y. Park, J. Phys. Chem. C 111 (2007) 4052–4060.
[11] C. Cuerva, J.A. Campo, M. Cano, C. Lodeiro, Chem. Eur. J. 22 (2016) 10168–10178.
[12] G. Levasseur-Thériault, C. Reber, C. Aronica, D. Luneau, Inorg. Chem. 45 (2006) 2379–2381.